Green Chemistry

COMMUNICATION

View Article Online
View Journal | View Issue

Cite this: *Green Chem.*, 2024, **26**, 11548

Received 9th September 2024,
Accepted 30th October 2024

DOI: 10.1039/d4gc04499a

rsc.li/greenchem

Continuous-flow synthesis of cyclic carbonates with polymer-supported imidazolium-based ionic liquid (Im-PSIL) catalysts†‡

Zhibo Yu,[a] Haruro Ishitani*[b] and Shu Kobayashi *[a,b]

Carbon dioxide (CO_2), a major greenhouse gas emitted through human activities, represents a valuable carbon source for chemical production. However, maximizing its efficient utilization requires novel methods for CO_2 conversion that leverage the advantages of heterogeneous catalysis in continuous-flow systems. Herein, we report polymer-supported ionic liquids (PSILs) as efficient and recyclable catalysts for the continuous-flow synthesis of cyclic carbonates from epoxides and CO_2. We designed imidazolium-based PSIL catalysts specifically for this purpose. These catalysts demonstrated remarkable stability for over 160 h under continuous-flow conditions with gaseous CO_2, achieving an average yield of over 90% throughout the reaction. Furthermore, they exhibit broad applicability to 12 different epoxide substrates, yielding moderate to excellent yields. This work suggests an environmentally friendly pathway for the sustainable and scalable production of cyclic carbonates.

Carbon dioxide (CO_2), a ubiquitous waste gas emitted in large quantities during industrial processes, agricultural production, and daily human activities, is paradoxically considered the ideal C1 source for producing organic chemicals due to its high availability, renewability, and non-toxic nature.[1] In 2022, CO_2 emissions were estimated to reach 36.8 billion tonnes, constituting approximately three-quarters of total greenhouse gas emissions.[2] This stands in stark contrast to the currently limited capture and storage capabilities. Therefore, capturing and utilizing CO_2 from industrial processes, particularly as a chemical feedstock, has recently gained global recognition as a critical strategy. This approach can contribute to both reducing greenhouse gases and transitioning away from a dependence on fossil resources.

Over the past few decades, the conversion of CO_2 into various organic chemicals has been extensively studied and optimized. Processes encompass a spectrum, ranging from converting simple molecules like methanol, urea, and formic acid through reductive processes to the production of high-value fine chemicals, including pharmaceuticals.[3–7] Among these successful applications, the synthesis of cyclic carbonates from epoxides and CO_2 has emerged as one of the most useful and well-studied non-reductive transformations.[8,9] This is due to their promising industrial applications as aprotic polar solvents and electrolyte solvents for lithium-ion batteries.[10,11] Additionally, cyclic carbonates are identified as benign intermediates for the synthesis of fine chemicals and pharmaceutical products.[12]

To overcome the low reactivity of CO_2 due to its inert nature and the high energy barriers in its interaction with epoxides, numerous catalysts and systems have been investigated and reported. These include well-designed metal complexes,[13–16] metal–organic frameworks (MOFs),[17,18] metalloporphyrins,[19] ionic liquids,[20–23] and halogen.[24] Among these, ionic liquids have attracted significant interest due to their typically strong affinity for CO_2 and the ease of structural modification, which allows for improved catalytic performance.[25,26] Additionally, incorporating carboxy- or hydroxy-functional groups onto the cationic moieties facilitates intramolecular hydrogen bonding with epoxides, promoting activation for the desired ring-opening reaction, resulting in enhanced catalytic activity.[21,27–29] Furthermore, the straightforward immobilization of ionic liquids onto suitable support materials offers advantages in terms of reusability and cost-effective production. Various modified support materials, such as silica gels,[27,30–33] polymers,[34–36] and zeolites,[37] have been reported to exhibit remarkable catalytic activity, designability, and stability.

Compared to conventional batch methods, continuous-flow methodology has attracted significant interest from researchers in both academia and industry, particularly for the preparation of fine chemicals like pharmaceuticals, agrochemicals,

[a]*Department of Chemistry, School of Science, The University of Tokyo, Hongo, Bunkyo-ku, Tokyo 113-0033, Japan. E-mail: shu_kobayashi@chem.s.u-tokyo.ac.jp*
[b]*Green & Sustainable Chemistry Social Cooperation Laboratory, Graduate School of Science, The University of Tokyo, Hongo, Bunkyo-ku, Tokyo 113-0033, Japan. E-mail: hishitani@chem.s.u-tokyo.ac.jp*

†Dedicated to Professor Koichi Narasaka on the occasion of his 80th birthday.

‡Electronic supplementary information (ESI) available. See DOI: https://doi.org/10.1039/d4gc04499a

polymers, and functional materials. In fact, continuous-flow methods have long been the standard in the petrochemical industry, proving to be the most efficient method for large-scale production.[38–44] While homogeneous micro- and flash-flow chemistry offers exceptional efficiency, especially in reactions involving short-lived active species,[45–48] the pursuit of carbon neutrality necessitates the development of heterogeneous catalytic processes for a broader range of chemical transformations under continuous-flow conditions.[49] Heterogeneous catalytic flow reactions enable the automatic separation of products from the catalyst bed along with the solvent. Additionally, the high catalyst-to-substrate ratio within the column enhances catalytic activity compared to corresponding batch reactions, leading to increased catalyst turnover number (TON). Precise control over residence time is achievable by adjusting flow rate and column size, preventing undesirable overreactions during the synthesis process.[50] Recent research from our group has demonstrated a remarkable acceleration effect, particularly for gas–liquid–solid reactions known as trickle-flow reactions, attributed to the direct contact of gas with the catalyst in the reactor bed.[51]

Turning to the synthesis of cyclic carbonates from CO_2, researchers have explored the transition from batch to continuous-flow methods for synthesizing cyclic carbonates from CO_2.[52–61] For instance, Xiong *et al*. employed carbon-tethered dialkyl imidazolium ionic liquids (ILs) for continuous-flow synthesis, achieving successful conversion of epichlorohydrin to the corresponding cyclic carbonate at 140 °C and 1.4 MPa with an average conversion of 82% over 80 h.[54] Recent studies by Sans and García-Verdugo,[58] Bica-Schröder,[59] and Yin[60] further demonstrate the versatility of this methodology. However, challenges remain in the continuous-flow synthesis of cyclic carbonates, including the occasional need for high pressure, limited reactivity, and a narrow substrate scope. Additionally, studies comparing the performance of heterogeneous catalysts in batch and continuous-flow systems have often revealed decreased yield and insufficient catalyst durability under continuous-flow conditions.[55–59,62,63] These findings suggest that the full potential of trickle-flow reactions has yet to be realized. Despite recent advances, high-productivity continuous-flow systems for cyclic carbonate synthesis still often rely on homogeneous catalysts, highlighting the challenges associated with using heterogeneous catalysts. For example, a benchmark study by Pericàs *et al.* employed immobilized amine catalysts for the synthesis of cyclic carbonates from glycerol derivatives, but the flow duration was limited to less than 48 h, and the turnover number (TON) was less than 100.[63] Simply anchoring active sites on a support appears insufficient for achieving high catalyst stability and activity.[64] We believe that directly modifying the polymer backbone is crucial for overcoming these limitations. In gas–liquid flow systems, the performance of heterogeneous catalysts can be significantly influenced by the positioning of polar active sites on the less-polar polymer backbone. To address this challenge, we prepared porous polymers with varying degrees of cross-linking in the presence of a porogen. By fine-tuning the active sites within these porous polymers, we developed catalysts suitable for continuous-flow cyclic carbonate synthesis with high stability (Fig. 1).

We initiated the design of a suitable polymer scaffold for gas–liquid–solid reactions and chose a styrene–divinylbenzene (DVB) backbone due to its synthetic scalability, chemical stability under reaction conditions, and affinity for both CO_2 and substrate solutions. Methyl isobutylcarbinol (MIBC) was used as a porogen, with its amount set at 90 wt% relative to the total monomer weight.[65,66] In this setup, the amount of cross-linking agent (DVB) relative to the other monomers was fixed at 8 wt%. To immobilize imidazolium moieties onto the scaffold, we adopted a post-modification method based on poly(4-vinylbenzyl bromide). Therefore, 4-vinylbenzyl bromide was used as a functionalized comonomer, and styrene served as the basic monomer. As outlined in Scheme 1, the installation of *N*-substituted imidazole, followed by anion exchange, provided the target butyl-tethered *N*-substituted imidazolium salt-functionalized porous polystyrene (**BRImPS**) catalysts. The bromide content in the polymer BBPS was determined by Volhard titration, and its structure was confirmed by infrared spectra and solid-state ^{13}C CP-MAS NMR (see S9 in ESI‡). The structure of **BHEImPS-4-890(Cl)** was also determined by comparison with that of the parent bromobutyl polystyrene using IR and ^{13}C CP-MAS NMR.

Initially, we evaluated the impact of the ratio between the basic monomer and the functionalized comonomer on performance in the cycloaddition reaction using styrene oxide (**1a**) under batch conditions (Table 1). In this study, we fixed several functionalities: (i) *N*-methylimidazole was used to construct the imidazolium moiety; (ii) the cross-linking degree, defined by the amount of DVB used, was fixed at 8 wt%; and (iii) the amount of porogen MIBC was set to 90 wt% as a standard, as described previously. In this manner, four **BMImPS-X-890(Br)** catalysts were prepared with stepwise increasing styrene proportions. Their differences manifested in a trend resembling a volcano shape in yields of the desired

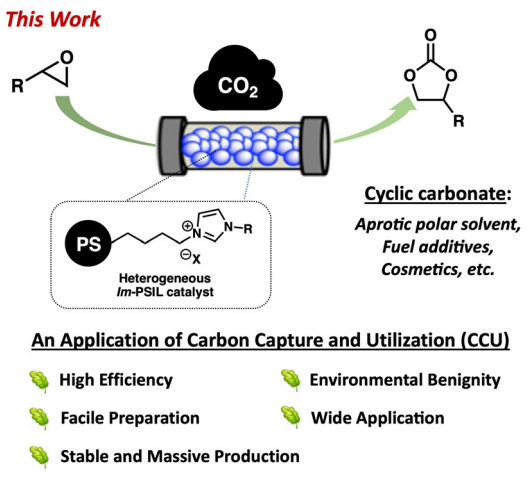

Fig. 1 General schematic image of this work.

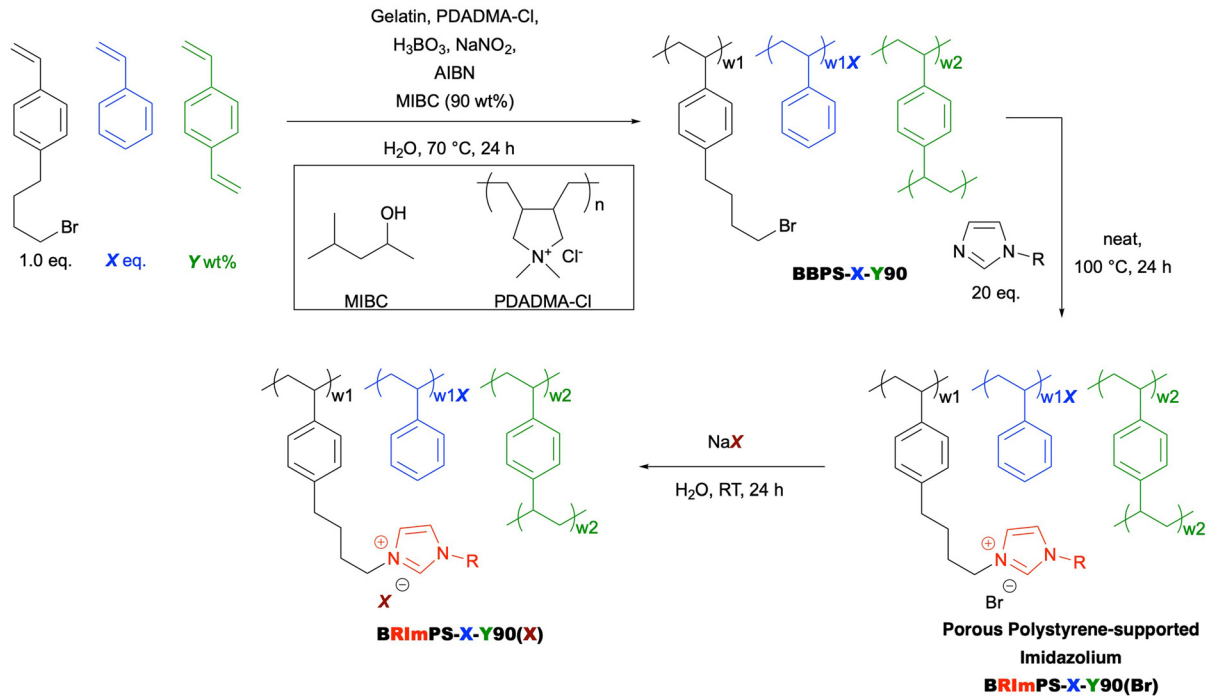

Scheme 1 Synthesis of polystyrene-supported imidazolium ionic liquid catalysts.

Table 1 Optimization of monomer/comonomer ratios for the cycloaddition reaction[a]

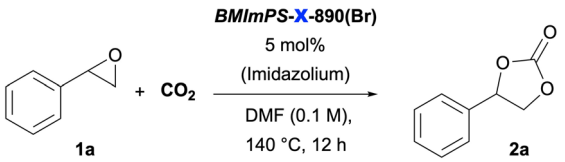

Entry	X^b [eq.]	Catalyst	Yield[c] [%]
1	0[d]	**BMImPS-0-890(Br)**	58
2	2	**BMImPS-2-890(Br)**	69
3	4	**BMImPS-4-890(Br)**	79
4	8	**BMImPS-8-890(Br)**	74
5	4	**BMImPS-4-800(Br)**[e]	66

[a] Conditions: **1a**, 1.0 mmol, CO_2, 1.0 MPa. [b] 4-Bromobutyl styrene/styrene ratio. [c] Determined by GC analysis. [d] The polymer that was prepared from 4-bromobutyl styrene and DVB. [e] The porogen was not used in the preparation of the catalyst.

styrene carbonate (2). Among them, **BMImPS-4-890(Br)**, where the number 4 indicates the mole-equivalency of styrene to the functionalized comonomer, showed the highest yield (79%).

Following the determination of the optimal monomer-to-comonomer ratio, we investigated the activity of **BMImPS-4-800(Br)** prepared without porogen. It exhibited a slightly lower yield of 66%. This highlights the importance of the porous structure for efficient substrate access to the catalytically active imidazolium moiety. One of the key advantages of this catalyst is its structural tunability, allowing for tailored catalytic performance for specific reactions. In this study, we extended our investigation beyond the polymer backbone by varying the spacer length between the polymer and the imidazolium group, as well as substituents on the imidazolium ring. A series of candidate catalysts are summarized in Fig. 2. Here, the monomer-to-comonomer ratio, crosslinking degree, and porogen amount were fixed at the optimal values determined previously. The corresponding counter anion is denoted at the end of each catalyst name. All prepared catalysts were evaluated under identical batch conditions in a model reaction, and the results are presented in Table 2.

BHImPS-4-890(Br), lacking an imidazolium substituent, displayed low catalytic activity (entry 1). Compared to the standard **BMImPS-4-890(Br)** (entry 2), shortening the alkyl linker between the polymer backbone and the imidazolium ring from C4 to C1 (**MMImPS-4-890(Br)**) resulted in decreased yield (entry 3). A similar trend was observed when the imidazolium substituent was changed to a 2-hydroxyethyl (HE) group: **BHEImPS-4-890(Br)** achieved an 87% yield (entry 6), whereas **MHEImPS-4-890(Br)** yielded only 58% (entry 8). This difference can be attributed to the influence of the hydrophobic polymer backbone, which may be more pronounced with a shorter alkyl linker.

During the exploration of various functional groups on the imidazolium nitrogen, the hydroxyethyl (HE) group provided the best performance (entry 6). Conversely, hydroxymethyl (HM) and hydroxypropyl (HP) groups significantly decreased the yield (entries 5 and 7). Previous studies have reported a similar positive effect of hydroxyl groups on the cycloaddition of CO_2 with epoxides to form cyclic carbonates, proposing

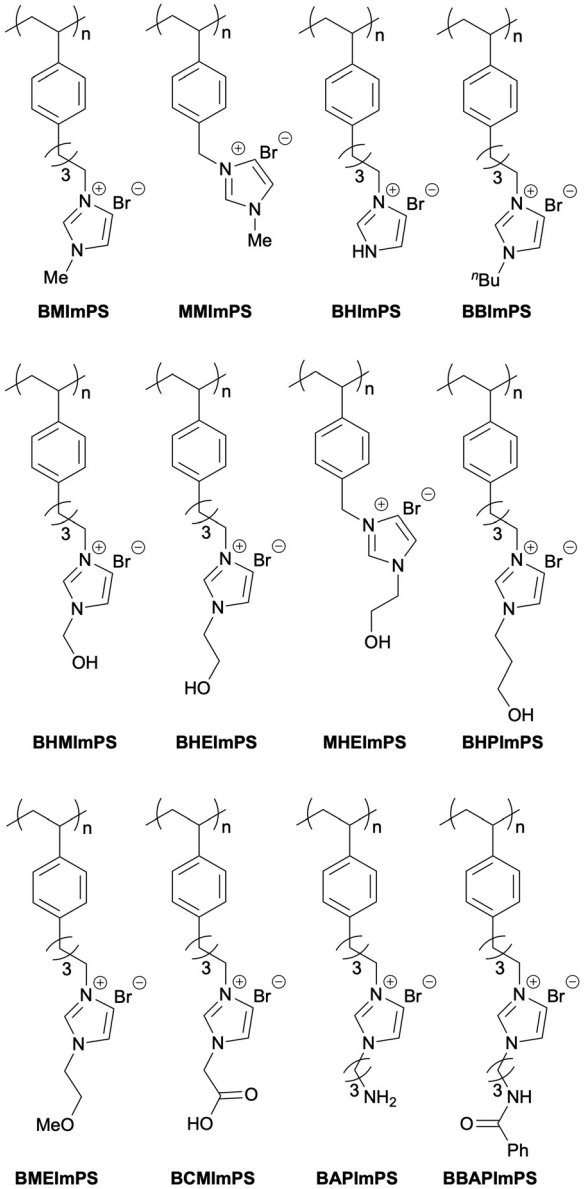

Fig. 2 Polystyrene-supported imidazolium ionic liquid catalysts.

hydrogen bonding between epoxides and the –OH group to activate the epoxide ring for subsequent C–O bond cleavage.[32,67–71] However, the negligible impact of HM and HP functionalities (entries 5 and 7) and the relatively better performance of methoxyethyl (ME) (entry 9) and also **BBImPS-4-890(Br)** (entry 4) suggest that hydrogen bond donation is not the critical factor for catalysis. This is further supported by the negative effect of other acidic functionalities like carboxymethyl (CM) and benzoyl aminopropyl (BAP) groups (entries 10 and 11). The aminopropyl (AP) substituent, capable of interacting with CO_2, also led to a decrease in yield (entry 12).

Further investigation focused on the anion component using variants of **BHEImPS-4-890**. The results in Table 2 (entries 13–20) indicate a strong influence of anion nucleophilicity on catalytic activity. The lowest yield observed with the least nucleophilic PF_6^- anion (entry 13) emphasizes the importance of nucleophilic character. Highly nucleophilic OH^- or moderately nucleophilic AcO^- resulted in yields of 40% or 57% (entries 19 and 20), possibly due to incompatibility with the hydroxyl group. Halide anions were effective, with yields increasing in the order $I^- < Br^- < Cl^-$ (entries 15–17). This effectiveness suggests that both appropriate nucleophilicity and leaving group ability are crucial for the catalytic cycle. Notably, **BHEImPS-4-890(Cl)**, an improved catalyst, achieved a 90% yield in the model batch reaction (entry 17). These results provide valuable insights into the reaction mechanism, which will be discussed further (*vide infra*).

Table 2 Catalytic ability of the series of prepared ionic liquid catalysts[a]

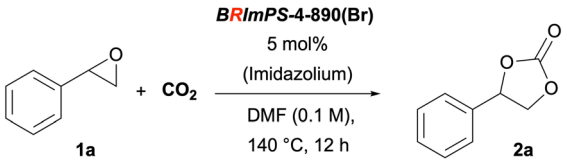

Entry	Catalyst	Yield[b] [%]
1	**BHImPS-4-890(Br)**	31
2	**BMImPS-4-890(Br)**	79
3	**MMImPS-4-890(Br)**	56
4	**BBImPS-4-890(Br)**	75
5	**BHMImPS-4-890(Br)**	53
6	**BHEImPS-4-890(Br)**	87
7	**BHPImPS-4-890(Br)**	70
8	**MHEImPS-4-890(Br)**	58
9	**BMEImPS-4-890(Br)**	82
10	**BCMImPS-4-890(Br)**	31
11	**BBAPImPS-4-890(Br)**	50
12	**BAPImPS-4-890(Br)**	55
13	**BHEImPS-4-890(PF_6)**	7
14	**BHEImPS-4-890(OTf)**	12
15	**BHEImPS-4-890(I)**	80
16	**BHEImPS-4-890(Br)**	87
17	**BHEImPS-4-890(Cl)**	90
18	**BHEImPS-4-890($OCOCF_3$)**	31
19	**BHEImPS-4-890(OH)**	40
20	**BHEImPS-4-890(OAc)**	57

[a] Conditions: **1a**, 1.0 mmol, CO_2, 1.0 MPa. [b] Determined by GC analysis.

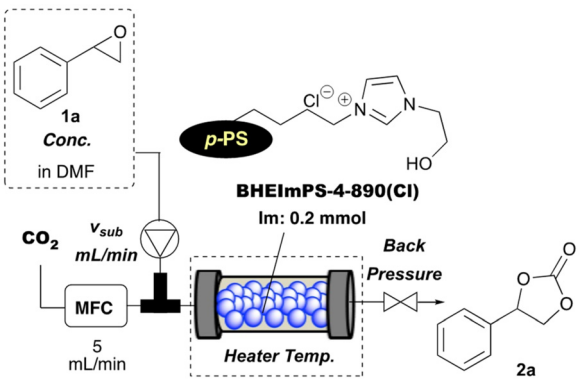

Scheme 2 Continuous-flow system.

With the optimal catalyst in hand, we further applied it in a continuous-flow system. The basic setup of our continuous-flow cycloaddition reaction is illustrated in Scheme 2. A 10 mm (id) × 200 mm (L) stainless steel plug-flow reactor containing 0.23 g of the catalyst **BHEImPS-4-890(Cl)** was installed in an aluminum block column heater. Under standard conditions consisting of a heater temperature of 140 °C and a back pressure of 0.5 MPa(G), we initiated our continuous-flow investigation by examining the effect of molar flow (F), the amount of substrate provided per unit time, which is a key parameter for flow reactions (Fig. 3. See also S-6 in ESI‡). In the first set of experiments, shown by the three bars on the left end of the line, decreasing the F value by reducing the flow rate from 0.1 mL min^{-1} to 0.025 mL min^{-1} resulted in a better yield of 72% at the lowest F value. The same yield was obtained under much higher pressure conditions; however, at this back pressure, conversely, better yields of 84 or 83% were obtained in operations with higher F, using a more concentrated substrate solution. Keeping the F value at 0.30 mmol h^{-1} and the catalyst amount constant, we employed a larger reactor to extend the residence time. Here, the estimated liquid resi-

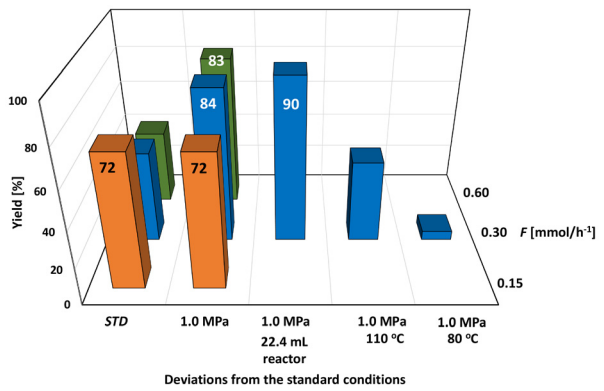

Fig. 3 Optimization of continuous-flow conditions.

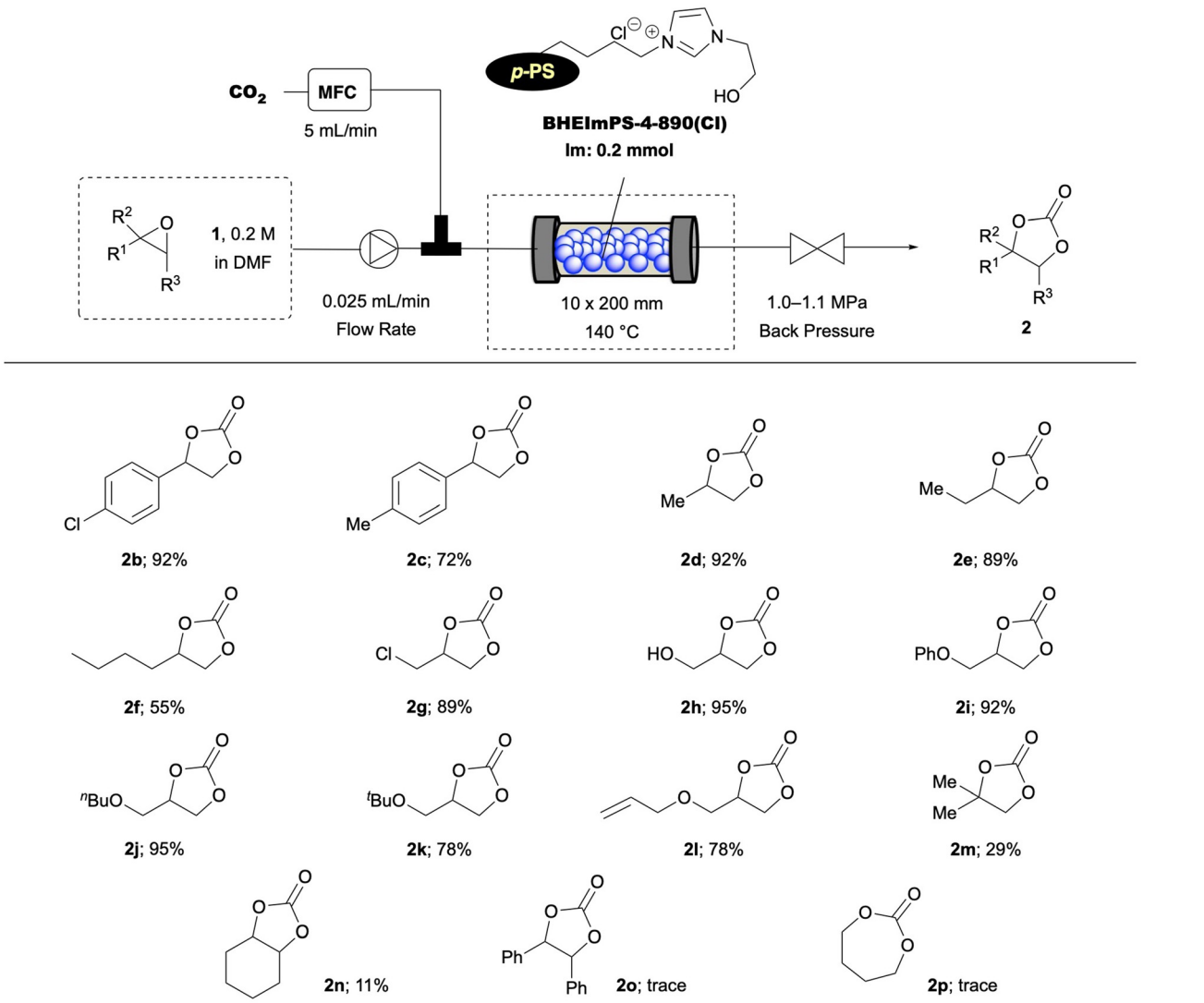

Fig. 4 Substrate scope in continuous-flow cyclic carbonate synthesis. Isolated yields except for **2n**, **2o**, and **2p** (determined by ^{1}H-NMR analysis).

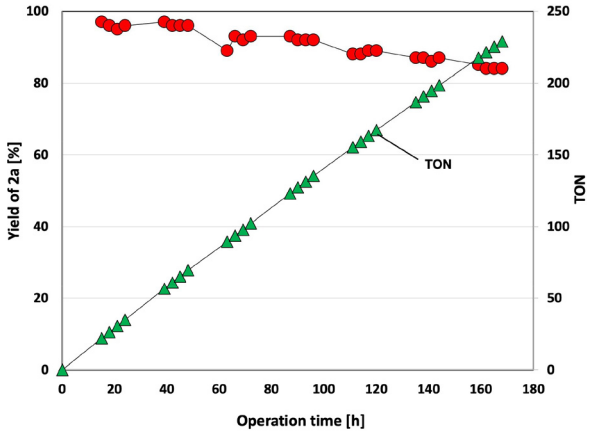

Fig. 5 Extended-time operation for the cycloaddition of **1a** and CO_2. Conditions: **1a**, 0.2 M; back pressure, 1.0–1.1 MPa; heater temp., 140 °C; 15.7 mL stainless reactor was utilized. Symbols: red circle, yield of **2a**; green triangle, TON based on the amount of imidazolium moiety in the reactor.

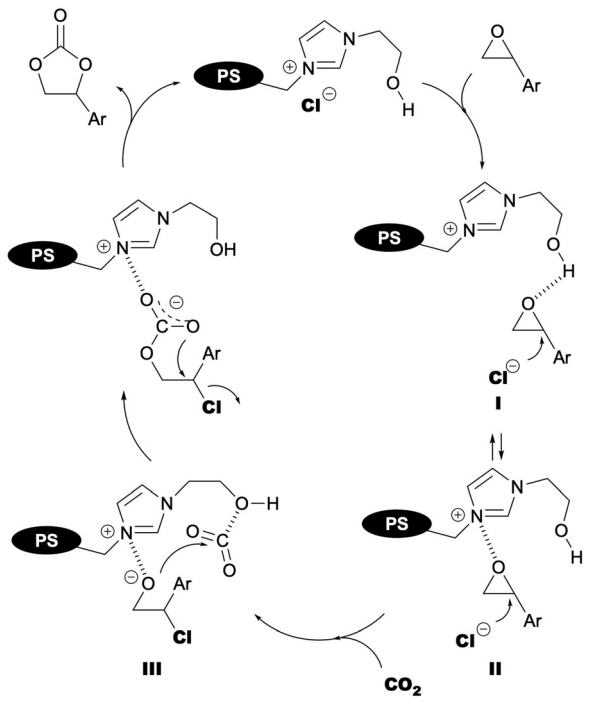

Fig. 6 Possible catalytic cycle.

dence time for the catalyst-packed reactors with inner volumes of 15.7 or 22.4 mL were 280 and 420 min, respectively. The yield of cyclic carbonate was increased to 90%. Trials to lower the column temperature from 140 °C to 110 or 80 °C resulted in lower product yields. To further reduce the environmental impact, we conducted the flow reaction under solvent-free conditions. Under the optimal conditions screened above, the yield of cyclic carbonate could reach 53%, and the STY value remained around 18 mmol h^{-1} dL. Having established the optimal flow conditions, we proceeded to explore the substrate scope of this system by using various epoxides. As demonstrated in Fig. 4, epoxides bearing mono-substituents readily underwent the reaction, yielding the desired products in good to excellent yields (72–96%), with the exception of 1-hexene oxide. A general trend can be observed: functional groups such as hydroxyl groups, ethers, and halogens were not affected in this reaction, and all resulted in high-yield products. We tested three types of styrene oxide derivatives with different electronic features, and found that only the electron-donating 4-methylstyrene oxide gave a slightly lower yield. Additionally, several di-substituted epoxides were examined as well; however, their low yields indicated their marked inactivity. Similarly, tetrahydrofuran (yielding **2p**) exhibited no activity in the reaction,[72] possibly due to the higher stability of the five-membered ring ether. We are actively working on expanding the applicability of our system to a wider range of substrates, including internal and *gem*-disubstituted epoxides.

The cycloaddition reaction between styrene oxide and CO_2 was investigated using **BHEImPS-4-890(Cl)** as a catalyst under extended operation time (Fig. 5). The estimated amount of catalytically active imidazolium sites in the reactor was 0.2 mmol. A 0.2 M solution of styrene oxide was continuously flowed at a rate of 0.025 mL min^{-1} (F = 0.3 mmol h^{-1}, SV = 1.5 h^{-1}). The CO_2 flow rate was maintained at 5 mL min^{-1}, and the back pressure was kept between 1.0 and 1.1 MPa(G). The reaction mixture was heated to 140 °C using an aluminum column heater and sustained for 168 h. The yield remained within the range of 84% to 97%, 91% yield in average, throughout the operation, demonstrating no significant activity loss. The estimated TON, exceeding 229, and the unchanged yield and turnover frequency (TOF) during the 180 h reaction highlight the high activity and exceptional stability of the catalyst, respectively.

The mechanism of the **BHEImPS-4-890(Cl)** catalyst-mediated cycloaddition between epoxide and CO_2 is proposed based on experimental results, assumptions, and insights from previous reports[32,69,70,73–78] and illustrated in Fig. 6. Hydrogen bonding between the epoxide oxygen and the hydroxyl group of the catalyst likely activates the epoxide (intermediate **I**), facilitating nucleophilic attack by the counter anion and subsequent ring opening. The resulting intermediate **III**, which possesses a highly nucleophilic alkoxide anion, then reacts with CO_2 to form a carbonate anion. Intramolecular nucleophilic attack within this intermediate completes the cyclization, leading to styrene carbonate formation. The effectiveness of imidazolium polymers lacking a hydroxyl group (*e.g.*, **BBImPS-4-890(Br)** and **BMEImPS-4-890(Br)**, see Table 2, entries 4 and 9) suggests the existence of an alternative catalytic mechanism that doesn't involve hydrogen bonding. This alternative mechanism likely relies on key features like the cationic imidazolium nitrogen and the nucleophilicity/leaving ability of the halides. Intermediate **II** in Fig. 6 represents a possible non-covalent interaction in this pathway. As mentioned earlier (Table 2), counter anions of the catalysts dramatically influenced their activities. According to the pro-

posed mechanism, halide anions with moderate nucleophilicity and leaving group ability, particularly chloride, exhibit superior catalytic activity. This behavior is consistent with the proposed mechanism. Further investigations into a more detailed reaction mechanism, including the rate-determining step, are ongoing.

In summary, this work showcases the application of meticulously optimized imidazolium-based ionic liquids immobilized on a polymer scaffold for the continuous-flow synthesis of cyclic carbonates from epoxides and CO_2. We prepared and evaluated a library of supported catalysts by varying the monomer/functionalized comonomer ratio, porogen amount, type of catalytically active moiety, and counterion. Among these, the **BHEImPS-4-890(Cl)** catalyst demonstrated outstanding catalytic performance. Continuous-flow experiments revealed its ability to efficiently produce various mono-substituted cyclic carbonates under optimized reaction conditions. Notably, extended operation for over 160 h maintained a consistent yield of over 90%, highlighting its exceptional stability. Future studies will focus on further enhancing catalytic activity and exploring its potential as a CO_2 conversion technology within the framework of Carbon Capture, Utilization, and Storage (CCUS).

Data availability

The data supporting this article have been included as part of the ESI.‡

Conflicts of interest

There are no conflicts to declare.

Acknowledgements

This work was supported in part by a Grant-in-Aid for Scientific Research from the New Energy and Industrial Technology Development Organization (NEDO) project Grant No. JPNP19004.

References

1 C. Hepburn, E. Adlen, J. Beddington, E. A. Carter, S. Fuss, N. MacDowell, J. C. Minx, P. Smith and C. K. Williams, *Nature*, 2019, **575**, 87–97.
2 International Energy Agency Report, CO_2 Emissions in 2022, https://www.iea.org/reports/co2-emissions-in-2022.
3 M. Peters, B. Köhler, W. Kuckshinrichs, W. Leitner, P. Markewitz and T. E. Müller, *ChemSusChem*, 2011, **4**, 1216–1240.
4 Y. Tsuji and T. Fujihara, *Chem. Commun.*, 2012, **48**, 9956–9964.
5 C. Maeda, Y. Miyazaki and T. Ema, *Catal. Sci. Technol.*, 2014, **4**, 1482–1497.
6 M. Usman, A. Rehman, F. Saleem, A. Abbas, V. C. Eze and A. Harvey, *RSC Adv.*, 2023, **13**, 22717–22743.
7 T. Ema, *Bull. Chem. Soc. Jpn.*, 2023, **96**, 693–701.
8 A.-A. G. Shaikh and S. Sivaram, *Chem. Rev.*, 1996, **96**, 951–976.
9 F.-T. Zangeneh, S. Sahebdelfar and T. T. Ravanchi, *J. Nat. Gas Chem.*, 2011, **20**, 219–231.
10 G.-C. Chung, H.-J. Kim, S.-H. Jun and M.-H. Kim, *Electrochem. Commun.*, 1999, **1**, 493–496.
11 Y. Hyun, H.-K. Park, H. S. Park and C.-S. Lee, *J. Nanosci. Nanotechnol.*, 2015, **15**, 8951–8960.
12 J. H. Clements, *Ind. Eng. Chem. Res.*, 2003, **42**, 663–674.
13 R. Srivastava, D. Srinivas and P. Ratnasamy, *Catal. Lett.*, 2003, **89**, 81–85.
14 Y.-M. Shen, W.-L. Duan and M. Shi, *Eur. J. Org. Chem.*, 2004, 3080–3089.
15 A. J. Kamphuis, F. Milocco, L. Koiter, P. P. Pescarmona and E. Otten, *ChemSusChem*, 2019, **12**, 3635–3641.
16 Q. Yao, Y. Shi, Y. Wang, X. Zhu, D. Yuan and Y. Yao, *Asian J. Org. Chem.*, 2022, **11**, e202200106.
17 O. V. Zalomaeva, A. M. Chibiryaev, K. A. Kovalenko, O. A. Kholdeeva, B. S. Balzhinimaev and V. P. Fedin, *J. Catal.*, 2013, **298**, 179–185.
18 Z. Gao, L. Kiang, X. Zhang, P. Xu and J. Sun, *ACS Appl. Mater. Interfaces*, 2021, **13**, 61334–61345.
19 T. Aida and S. Inoue, *J. Am. Chem. Soc.*, 1983, **105**, 1304–1309.
20 W.-L. Wong, L. Y. K. Lee, K.-P. Ho, Z.-Y. Zhou, T. Fan, Z. Lin and K.-Y. Wong, *Appl. Catal., A*, 2014, **472**, 160–166.
21 C. Yue, D. Su, X. Zhang, W. Wu and L. Xiao, *Catal. Lett.*, 2014, **144**, 1313–1321.
22 S. Yue, P. Wang and X. Hao, *Fuel*, 2019, **251**, 233–241.
23 C. Li, F. Liu, T. Zhao, J. Gu, P. Chen and T. Chen, *Mol. Catal.*, 2021, **511**, 111756.
24 J. A. Kozak, J. Wu, X. Su, F. Simeon, T. A. Hatton and T. F. Jamison, *J. Am. Chem. Soc.*, 2013, **135**, 18497–18501.
25 C. Cadena, J. L. Anthony, J. K. Shah, T. I. Morrow, J. F. Brennecke and E. J. Maginn, *J. Am. Chem. Soc.*, 2004, **126**, 5300–5308.
26 A. S. Martinez, C. Hauzenberger, A. R. Sahoo, Z. Csendes, H. Hoffmann and K. Bica, *ACS Sustainable Chem. Eng.*, 2018, **6**, 13131–13139.
27 W.-L. Dai, L. Chen, S.-F. Yin, W.-H. Li, Y.-Y. Zhang, S.-L. Luo and C.-T. Au, *Catal. Lett.*, 2010, **137**, 74–80.
28 S. Wu, B. Wang, Y. Zhang, E. H. M. Elageed, H. Wu and G. Dao, *J. Mol. Catal. A: Chem.*, 2016, **418–419**, 1–8.
29 T. Wang, X. Zhu, L. Mao, T. Ren, L. Wang and J. Zhang, *J. Mol. Liq.*, 2019, **296**, 111936.
30 W.-L. Dai, L. Chen, S.-F. Yin, S.-L. Luo and C.-T. Au, *Catal. Lett.*, 2010, **135**, 295–304.
31 W. Cheng, X. Chen, J. Sun, J. Wang and S. Zhang, *Catal. Today*, 2013, **200**, 117–124.
32 T. Ying, Q. Su, Z. Shi, L. Deng, W. Cheng and W. Hua, *Catal. Lett.*, 2019, **149**, 2647–2655.
33 A. Siewniak, A. Forajter and K. Szymanska, *Catalysts*, 2020, **10**, 1363.

34 L. Han, H.-J. Choi, D.-K. Kim, S.-W. Park, B. Liu and D.-W. Park, *J. Mol. Catal. A: Chem.*, 2011, **338**, 58–64.
35 Y. Zhang, E.-S. M. El-Sayed, K. Su, D. Yuan and Z. Han, *J. CO_2 Util.*, 2020, **42**, 101301.
36 W. Zhang, F. Ma, L. Ma, Y. Zhou and J. Wang, *ChemSusChem*, 2020, **13**, 341–350.
37 L. Guo, X. Jin, X. Wang, L. Yin, Y. Wang and Y.-W. Yang, *Molecules*, 2018, **23**, 2710.
38 L. D. Elliott, J. P. Knowles, P. J. Koovits, K. G. Maskill, M. J. Ralph, G. Lejuene, L. J. Edwards, R. I. Robinson, I. R. Clemens, B. Cox, D. D. Pascoe, G. Koch, M. Eberle, M. B. Berry and K. I. Booker-Milburn, *Chem. – Eur. J.*, 2014, **20**, 15226–15232.
39 I. R. Baxendale, R. D. Braatz, B. K. Hodnett, K. F. Jensen, M. D. Johnson, P. Sharratt, J.-P. Sherlock and A. J. Florence, *J. Pharm. Sci.*, 2015, **104**, 781–791.
40 S. Kobayashi, *Chem. – Asian J.*, 2016, **11**, 425–436.
41 H. Ishitani, Y. Saito and Y. S. Kobayashi, *Top. Organomet. Chem.*, 2016, **57**, 213–248.
42 M. Kandasamy, B. Ganesan, M.-Y. Hung and W.-Y. Lin, *Eur. J. Org. Chem.*, 2019, 3183–3189.
43 W. J. Yoo, H. Ishitani, Y. Saito, B. Laroche and S. Kobayashi, *J. Org. Chem.*, 2020, **85**, 5132–5145.
44 S. B. Ötvös and C. O. Kappe, *Green Chem.*, 2021, **23**, 6117–6138.
45 J. Yoshida, *Flash Chemistry - Fast Organic Synthesis in Micro Systems*, WILEY-VCH, Weinheim, 2008.
46 J. Yoshida, A. Nagaki and T. Yamada, *Chem. – Eur. J.*, 2008, **14**, 7450–7459.
47 J. Yoshida, *Chem. Rec.*, 2010, **10**, 332–341.
48 J. Yoshida, Y. Takahashi and A. Nagaki, *Chem. Commun.*, 2013, **49**, 9896–9904.
49 M. B. Plutschack, B. Pieber, K. Gilmore and P. H. Seeberger, *Chem. Rev.*, 2017, **117**, 11796–11893.
50 S. G. Newman and K. F. Jensen, *Green Chem.*, 2013, **15**, 1456–1472.
51 S. Asano, H. Miyamura, M. Matsushita, S. Kudo, S. Kobayashi and J.-I. Hayashi, *J. Flow Chem.*, 2023, **14**, 329–335.
52 H. Seo, L. V. Nguyen and T. F. Jamison, *Adv. Synth. Catal.*, 2019, **361**, 247–264.
53 A. Rehman, F. Saleem, F. Javed, A. Ikhlaq, S. W. Ahmad and A. Harvey, *J. Environ. Chem. Eng.*, 2021, **9**, 105113.
54 Y. Zhang, Z. Tan, B. Liu, D. Mao and C. Xiong, *Catal. Commun.*, 2015, **68**, 73–76.
55 T. Wang, W. Wang, Y. Lyu, X. Chen, C. Li, Y. Zhang, X. Song and Y. Ding, *RSC Adv.*, 2017, **7**, 2836–2841.
56 A. S. Martinez, C. Hauzenberger, A. R. Sahoo, Z. Csendes, H. Hoffmann and K. Bica, *ACS Sustainable Chem. Eng.*, 2018, **6**, 13131–13139.
57 D. Valverde, P. Porcar, P. Lozano, E. García-Verdugo and S. V. Luis, *ACS Sustainable Chem. Eng.*, 2021, **9**, 2309–2318.
58 D. Valverde, P. Porcar, M. Zanatta, S. Alcalde, B. Altaba, V. Sans and E. García-Verdugo, *Green Chem.*, 2022, **24**, 3300–3308.
59 P. Mikšovsky, E. N. Horn, S. Naghdi, D. Eder, M. Schnürch and K. Bica-Schröder, *Org. Process Res. Dev.*, 2022, **26**, 2700–2810.
60 X. Li, J. Sun, M. Xue and J. Yin, *J. CO_2 Util.*, 2022, **64**, 102168.
61 T. Q. Bui, L. J. Konwar, A. Samikannu, D. Nikjoo and J.-P. Mikkola, *ACS Sustainable Chem. Eng.*, 2020, **8**, 12582–12869.
62 N. Zanda, L. Zhou, E. Alza, A. W. Kleij and M. À. Pericàs, *Green Chem.*, 2022, **24**, 4628–4633.
63 N. Zanda, A. Sobolewska, E. Alza, A. W. Kleij and M. À. Pericàs, *ACS Sustainable Chem. Eng.*, 2021, **9**, 4391–4397.
64 C. Mizyka, S. Renson, B. Grignard, C. Detrembleur and J.-C. M. Monbaliu, *Angew. Chem., Int. Ed.*, 2024, **63**, e202319060.
65 M. Tomoi and W. T. Ford, *J. Am. Chem. Soc.*, 1981, **103**, 3828–3832.
66 Y.-F. Wang, B.-H. Xu, Y.-R. Du and S.-J. Zhang, *Mol. Catal.*, 2018, **457**, 59–66.
67 J. Sun, S. Zhang, W. Cheng and J. Ren, *Tetrahedron Lett.*, 2008, **49**, 3588–3591.
68 J. Sun, W. Cheng, W. Fan, W. Wang, Z. Meng and S. Zhang, *Catal. Today*, 2009, **148**, 361–367.
69 X. Chen, J. Sun, J. Wang and W. Cheng, *Tetrahedron Lett.*, 2012, **53**, 2684–2688.
70 M. Zhang, B. Chu, G. Li, J. Xiao, H. Zhang, Y. Peng, B. Li, P. Xie, M. Fan and L. Dong, *Microporous Mesoporous Mater.*, 2019, **274**, 363–372.
71 Y. Liu, J. Li, Z. Zhang, Y. Hou and J. Zhang, *Inorg. Chem.*, 2022, **61**, 17438–17447.
72 E. Jie and W. Zhang, CN103058862A, 2012.
73 D.-W. Kim, R. Roshan, J. Tharun, A. Cherian and D.-W. Park, *Korean J. Chem. Eng.*, 2013, **30**, 1973–1984.
74 V. B. Saptal and B. M. Bhanage, *Curr. Opin. Green Sustainable Chem.*, 2017, **3**, 1–10.
75 A. A. Marciniak, K. J. Lamb, L. P. Ozorio, C. J. A. Mota and M. North, *Curr. Opin. Green Sustainable Chem.*, 2020, **26**, 100365.
76 M. Liu, F. Wang, L. Shi, L. Liang and J. Sun, *RSC Adv.*, 2015, **5**, 14277–14285.
77 S. Denizalti, *RSC Adv.*, 2015, **5**, 45454–45458.
78 Z. Guo, Y. Hu, S. Dong, L. Chen, L. Ma, Y. Zhou, L. Wang and J. Wang, *Chem. Catal.*, 2022, **2**, 519–530.